Connection between urban heat island and sky view factor approximated by a software tool on a 3D urban database

János Unger

Department of Climatology and Landscape Ecology,
University of Szeged,
P.O. Box 653, Szeged H-6701, Hungary
E-mail: unger@geo.u-szeged.hu

Abstract: This study provides a review on methods of Sky View Factor (SVF) determination and intra-urban surface geometry–air temperature relationship. Then, a software-based method of SVF estimation from a 3D database, describing urban surface elements, is applied. Finally, related investigations in Szeged and importance of the results obtained are discussed. Previous investigations were limited to only specific urban parts or some canyons and used small numbers of sites and few occasions of measurements. This study utilises a large number of areal means of SVF and temperature related to a large sample area and based on numerous measurements. Our investigation reveals a strong relationship between these variables. Thus, surface geometry is a significant determining factor of the temperature distribution if the selected scale is appropriate. Therefore, investigations of sufficient number of appropriate-sized areas, covering large parts of a city, are needed to draw well-established conclusions on the studied relationship.

Keywords: 3D urban database; sample area; SVF; sky view factor; computer algorithm; UHI; urban heat island; linear regression; Szeged; Hungary.

Reference to this paper should be made as follows: Unger, J. (2009) 'Connection between urban heat island and sky view factor approximated by a software tool on a 3D urban database', *Int. J. Environment and Pollution*, Vol. 36, Nos. 1/2/3, pp.59–80.

Biographical notes: János Unger is an Associate Professor in the Department of Climatology and Landscape Ecology, University of Szeged, Hungary. He received a Master's degree in Mathematics and Geography and a PhD in Climatology. He is teaching general climatology, environmental climatology, urban climatology and cartography. His research interests are urban climatology, especially the temperature excess generated by built-up areas and its connection to surface geometry and land use types, as well as human bioclimatology in different urban micro-environments.

1 Introduction

Urban environments appear as uneven artificial terrains with building materials partly different from those of natural surfaces. In addition, anthropogenic processes release excess heat and pollution to the ambient air. These alterations modify the energy and water balance, which often results in higher urban temperature compared to the relatively natural surroundings – this is the so-called Urban Heat Island (UHI). Generally, its strongest development occurs at night when the heat, stored in the daytime, is released (Kuttler, 2005; Landsberg, 1981; Oke, 1987). The UHI intensity (ΔT) for a given urban location is defined as the difference between the air or surface temperatures of that urban site and those of a carefully selected nearby non-urban (reference) site or those of a mean of non-urban sites (e.g. Lowry, 1977). The intensity of the UHI depends strongly on the land use and urban parameters (e.g. built-up ratio, green surface ratio, Sky View Factor (SVF), etc.) characterising the immediate environment of the site of the measurement (e.g. Golany, 1996; Oke, 1987; Unger et al., 2004).

Nocturnal cooling processes are primarily forced by outgoing long-wave radiation. In cities, narrow streets and high buildings create deep canyons. This 3D geometrical configuration plays an important role in regulating long-wave radiation heat loss. Due to the fact that only a smaller part of the sky is seen from the surface (because of the horizontal and vertical unevenness of the surface elements), the outgoing long-wave radiation loss here is more restricted than in rural areas.

The intra-urban distribution of the temperature excess is largely dependent on local surface characteristics, such as building heights (H) and street (canyon) width or spaces between buildings (W). The H/W ratio describes how densely spaced buildings are with respect to their heights. Together with the growing values of H/W, an increasingly large portion of the cold sky is replaced with the relatively warm flanks of buildings. A more appropriate measure of the radiation geometry of a given site is its SVF, that is, the ratio of the radiation received (or emitted) by a planar surface to the radiation emitted (or received) by the entire hemispheric environment (Watson and Johnson, 1987). It is a dimensionless measure between zero and one, representing totally obstructed and free spaces, respectively (Oke, 1988). SVF is determined for a specific point in space, that is, it gives a measure of the openness of the sky to radiative transport relative to a specific location. Its advantage over other geometric measures like H/W is that a complex urban environment can be described much better (Johnson and Watson, 1984). Below roof level the decreased SVF reduces radiative loss and besides, in the case of light gradient wind it also reduces turbulent heat transfer in the often calm canyon air. Therefore, theoretically it is considered to be one of the major agents of the UHI phenomenon.

In the determination of the spatial features of the urban structure, the application of geoinformatical methods could be very useful. Urban geometry can be reasonably modelled well using a 3D database with fine resolution and this database can be a source of geoinformatical evaluations with different aims.

The first objective of this paper is to provide a comprehensive review on methods directed to SVF determination in complex environments and on intra-urban surface geometry–air temperature relationships found in the literature. The second objective is to apply a software-based method similar to Souza et al. (2003, 2004) for the SVF estimation from a 3D database, describing and quantifying urban surface geometric elements. The third objective is to contribute to this context by related investigations in Szeged, located in south-east Hungary, especially to present the recent development and the importance of results obtained compared to the previous studies.

2 Definition of SVF, its physical interpretation and calculation

A View Factor (VF) is a geometric ratio that expresses the fraction of the radiation output from one surface (A) that is intercepted by another (B). It is a dimensionless number between 0 and 1 and is marked with VF_{A-B}. More detail is given in Oke (1987) and Brown and Grimmond (2001).

Taking a point of the urban surface, one part of the radiation from the point is absorbed on the surfaces around the point (buildings, trees, etc.) and the remaining part is directed to the sky. The measure of this part is defined as the SVF, which means that the value of SVF can be calculated by subtracting from 1 the sum of all the VFs calculated for the surfaces 'seen' from the point.

In urban environments, the SVF is determined predominantly by buildings as the main elements of this surface. Therefore, in the further parts of the study 'urban surface' means only the ensemble of building surfaces and horizontal surfaces at ground level situated in the city.

Thus, one part of the sky is obstructed by the buildings and the remaining part is visible. Theoretically, viewing a given surface element (ΔA), the part of the sky obstructed by buildings can be determined by projecting each building on a hemisphere representing the sky with projecting lines (Figure 1). The surface marked by S_B on the hemisphere shows the shape of the building 'seen' from ΔA. In this case the SVF is:

$$\mathrm{SVF} = 1 - \mathrm{VF}_{\mathrm{building}-\Delta A} = 1 - \mathrm{VF}_{S_B - \Delta A}$$

Figure 1 Projection of a building (S_B) 'seen' from a surface element (ΔA) on a hemisphere centred on ΔA

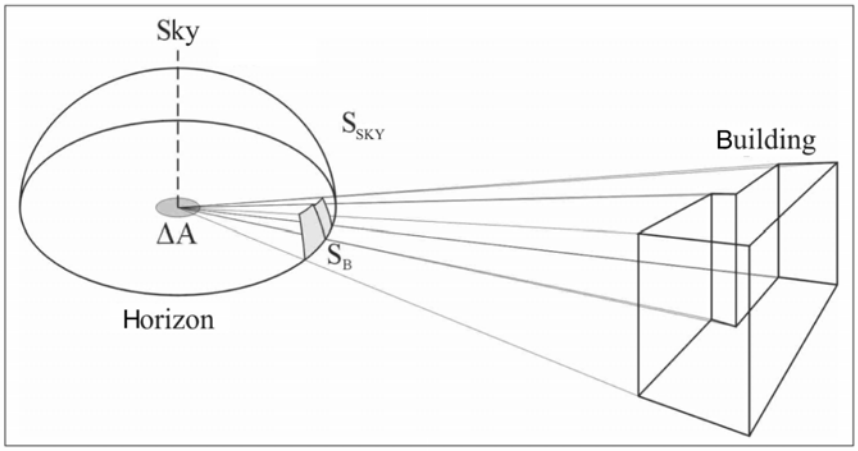

Some very simplified SVFs for common geometric arrangements are given in Oke (1987). Figure 2 shows the case of the basin, where the vertical extension (depth) and the distance from the ellipse centre are marked by H and W, respectively, while β means the elevation angle. The SVF value in this special case (referring to the centre marked by ellipse on Figure 2) is given as follows:

$$\mathrm{SVF}_{\mathrm{basin}} = \cos^2 \beta \tag{1}$$

Figure 2 Geometrical arrangements of the basin (H = height, W = width, β = elevation angle)

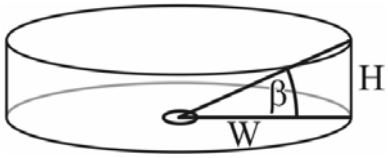

Source: Oke (1987).

3 Determination of SVF in urban environment, UHI–SVF relationship (review)

Surveying the related literature, one can find several papers dealing, at least partly, with the evaluation methods for SVF and with the relationship between the screen level (air) temperature or UHI intensity (ΔT) and SVF. In the following the results of some important investigations are summarised.

3.1 Methods for SVF determination

The methods directed to the estimation or calculation of SVF in urban environment (partly in natural environment) can be classified as follows:

- scale model (Oke, 1981)
- analytical method (angle measurements, H/W), estimation by graphics (e.g. Bottyán and Unger, 2003; Johnson and Watson, 1984; Watson and Johnson, 1987)
- manual and computer evaluation of fisheye photos (e.g. Blankenstein and Kuttler, 2004; Bradley et al., 2001; Brown and Grimmond, 2001; Chapman et al., 2001; Grimmond et al., 2001; Holmer, 1992; Holmer et al., 2001; Steyn, 1980) (see Figure 3)
- evaluation of GPS signals (Chapman and Thornes, 2004; Chapman et al., 2002)
- computer evaluation of a 3D database describing surface geometric elements (e.g. Brown et al., 2001; Lindberg, 2004; Souza et al., 2003).

Figure 3 A fisheye photograph in an urban area of Szeged (NIKON Coolpix 4500 camera with FC-E8 fisheye lens)

In order to avoid repetitions, detailed review of methods and results will be made only in the case of those works, which are not discussed in Unger (2004).

An analytical method for the determination of VFs for single buildings was given by Johnson and Watson (1984). Later they also gave nomograms for the estimations of such factors (Watson and Johnson, 1987). Their calculation needs only the elevation and azimuth angles of a building and knowing these two angles the SVF value can be read from the nomogram.

An alternative approach to estimate VFs is the use of fisheye photographs. Steyn (1980) introduced a method to get a geometrically correct SVF of fisheye image for use in complex urban environments. He divided the image into 37 concentric annuli and measured the sum of sky arcs in each annulus. The SVF is the total of these sums multiplied by a weighting factor. In the interests of the fast and exact process (aiming the distinction of the sky from surface elements), different fisheye image evaluation methods were developed for use before the final preparation. Traditionally, printed copies of images were analysed manually using polar coordinate graph paper, which was time-consuming and subject to error. Firstly, experiments for automation of these methods have involved digitising the fisheye images with a video camera (Bärring et al., 1985) or direct collection of imagery with a video camera fitted with a fisheye lens (Steyn et al., 1986). Holmer (1992) evaluated the fisheye photos in small sectors by a digitising tablet connected to a computer. The precision and process time were dependent on sector width.

Grimmond et al. (2001) first applied a digital camera with a fisheye lens, then a plant canopy analyser to measure diffused non-interceptance light using a fisheye optical sensor. The digital camera provides accurate estimates of SVF (using a purpose written Fortran program), while the canopy analyser tends to overestimate it. For both methods, data collection and post-processing is rapid, thus mobile measurements are possible which allow for detailed information on the spatial variability in a given urban area. Brown and Grimmond (2001) used fisheye image analysis to alter the brightness and contrast and then the above-mentioned in-house processing software to compute SVF. Chapman et al. (2001) presented a fully automated digital approach to distinguish the sky from non-sky using greyscale digital numbers on the converted fisheye images. They developed the calculation of SVF from the work of Steyn (1980). Similar methods were applied by Holmer et al. (2001) in the case of forest canopies.

One of the interesting problems are the estimation of urban canyon dimensions over wider areas. It is possible to acquire data sets with individual buildings but few data exist for cities. Bradley et al. (2001) offer a solution using the method of Chapman et al. (2001) for SVF calculation for the points in sample transects through different land cover classes. Their statistical analysis of the obtained SVF databases by classes opened possibilities for more detailed SVF estimation over wide areas of land cover types, which could be very useful for urban climate modelling.

A recent technique allows the real-time measurement of SVF using a GPS receiver to acquire satellite visibility data (Chapman et al., 2002). The number of satellites, dilution of precision and strength of satellite signal are used to develop multiple regression equations for the prediction of the SVF of a location. They give good results in urban environments, but in rural and suburban environments where trees produce noisy and highly variable data sets over short distances, the validity of prediction is reduced. This fast process enables the measurement of SVF in transects over larger areas. The GPS proxy technique was further developed by Chapman and Thornes (2004) to provide

instant calculation of SVF for application in mobile platform with a processing time of 1 s. In their study, three GPS parameters were chosen for analysis: the number of tracked satellites, the number of visible satellites and the sum of signal-to-noise ratios. The model prediction of SVF was performed by an artificial neural network. The model was tested by comparing with SVF values calculated by a real-time fisheye image process. The application of SVF calculation based on GPS signals is not restricted for 'ideal' weather conditions as fisheye image processes, where the imagery must be collected during the consistent light levels found during 'ideal' homogenous cloudy conditions.

A relatively new approach is the construction of a raster database covering the investigated area and the SVF is computed by repeatedly casting shadows on building data sets (Brown et al., 2001). The output is a black and white image, which shows the amount of light and shadow for each point. It is extremely fast and can process large areas of a city at one time, but the applied raster data base had a rather coarse resolution (2 m/pixel). Lindberg (2004) utilises similar process for deriving SVF based on an urban Digital Elevation Model (pixel resolution of 0.5 m) converted from a vector-based raw municipality database with an accuracy and precision of 0.01 m. Their process and the method based on fisheye images were compared with satisfactory results.

For the SVF estimation, Souza et al. (2003, 2004) developed an extension called 3DSkyView, which works in an environment created by ArcView GIS version 3.2 with its 3D Analyst extension (www.esri.com). The plan areas of buildings were available as a polygon layer with heights of buildings in the attribute table. A stereographic projection (it is not similar to a fisheye photograph!) on a 2D plane was applied to identify a new coordinate system for the 3D elements. The determination of SVF of a given point is then just a question of the spatial manipulation of layers by overlaying a stereonet of equal radius on the stereographic projection of the scene and comparing the area occupied by buildings and sky area.

3.2 UHI–SVF relationships

Concerning the relationship between the UHI and SVF in urban environments, a question arises: How strong is the connection between the air temperature and the SVF? Or can real connection be detected only with the surface temperature? According to the related literature, the variation of surface temperature can be explained to a great extent with the variation of SVF (Unger, 2004). In the case of air temperature, the results obtained related to SVF–ΔT are rather contradictory, since the relationship appears sometimes strong and sometimes weak depending on the investigations. Previous investigations were limited to the centre or only specific parts or only some urban canyons of cities (e.g. Eliasson, 1996; Park, 1987), and used small numbers of sites and few occasions of measurements (e.g. Goh and Chang, 1999; Park, 1987). Therefore, any examination of possible connections were also based on a small number of element pairs. Comparisons were often based on element pairs measured at some selected sites (e.g. Johnson, 1985; Upmanis et al., 1998). In some cases, we meet with areal means as well, but only in the case of one of the examined variables (e.g. Goh and Chang, 1999; Oke, 1981; Vieira and Vasconcelos, 2003).

In a recent paper (Svensson, 2004), air temperature was collected at 16 sites at a height of 2 m in different land use categories (36 occasions) and by car traverses

(2 occasions) in the urban area of Göteborg during clear, calm nights for 3 hr after sunset. SVF values in each station at both sensor height and ground level were calculated from the fisheye photographs using a method developed by Holmer et al. (2001). The results obtained by regression analysis indicate a fairly strong relationship between SVF and ΔT, especially within the same land use category (R^2 = 0.78). Data from permanent stations show that it is better to use the SVF values belonging to the points at ground level for regression analysis than values that belong to the elevated points.

In contrast to the earlier-mentioned studies, Blankenstein and Kuttler (2004) and Unger (2004) applied a different approach to investigate SVF–UHI relation since their works are based on areal means for every investigated parameter.

In Szeged, Hungary the SVF values can be regarded as estimations of the real-SVF values, because an analytical method was applied where two elevation angles to the top of buildings were measured normal to the axis of streets in both directions, using a 1.5 m high theodolite (Bottyán and Unger 2003; Unger, 2004). SVF was determined along the measuring routes used for temperature sampling. About 532 points were surveyed and the SVF data obtained were averaged by cells. Unger (2004) used a large number of cell averages of SVF and ΔT as element pairs. The relationship between SVF and the one-year average of ΔT calculated from 35 night measurements was examined. According to the statistical measures obtained, the intra-urban variations of temperature excess can be explained by the variations in SVF of 47%. The correlation coefficient indicated a strong negative relationship at the 1% significance level. Then, the relationships in the leaf-off and the leaf-on seasons were studied separately. According to the comparison between the colder and warmer half-years, the connection was stronger in the colder season than in the warmer, but the difference was not too large. The correlation coefficients indicated negative relationships, which mean only a difference of 4% in the explanation of ΔT variation caused by the variation of SVF.

Blankenstein and Kuttler (2004) applied similar approach averaging their temperature and SVF data by defined sections of the measurement route. They analysed the interrelation between the SVF, downward long-wave radiation and air temperature in an urban environment of Krefeld, Germany. The parameters were measured by car traverses during seven clear and calm summer nights with a 10–20-m sampling frequency. As for the SVF values, fisheye photographs (taken at 1.6 m agl) were evaluated with the Fortran program (Grimmond et al., 2001) mentioned in Section 3.1. The traverse was divided into sections with only building, with only vegetation and mixed, and then section averages of the measured parameters were calculated. The correlation of long-wave radiation and SVF was strong with a coefficient of determination of 0.91, but the ΔT was weakly correlated with the SVF.

4 Algorithm of the SVF calculation

As mentioned earlier, the purpose was to develop an algorithm, which is able to determine the SVF for an optional point using a 3D building database. Therefore, the quality of the 3D database determines considerably the accuracy of the calculation algorithm. This database is a model of the real world, which represents a simplified (containing buildings only) urban surface.

4.1 Applied 3D database

4.1.1 Creation of the 3D database

Raster basis: 30 pieces of overlapping (60%) aerial photographs from 1992 cover the city of Szeged. The negatives were digitised in a scanner (14 micron resolution).

Vector basis (digital map): the plan areas of buildings were available in DXF format as a polygon layer. The mean error of the vector data is 10 cm, therefore its accuracy can be considered geodesic. Buildings with an area of less than 15 square metres were omitted from the study, since these small buildings are difficult to determine on the aerial photos, and their heat absorption and emission are negligible.

Software: ERDAS IMAGINE (applied modules: OrthoBASE, Stereo Analyst and VirtualGIS), ESRI ArcView and Xtools extension.

1:10,000 scale maps: Geodesic-topographic maps of the Unified National Mapping System (in Hungarian EOTR): No. 27-323, 27-332, 27-341, 27-342 and 27-343.

Digital Elevation Model (DEM): DEM is a general spatial model, which represents a bare surface without landmarks. In case of Szeged, the vertical variation of the surface is small (75.5–83 m asl), so using a DEM enabled us to increase the accuracy of the orthophoto. After digitising the 1:10,000 scale maps the contour lines were vectorised in ERDAS IMAGINE, then the DEM of this area was created. This DEM was used for the preparation of the orthophotos and the visual representation of the model in VirtualGIS. Both vector and raster data are in the Unified National Projection (EOV in Hungarian) so they exactly overlap each other (layer structure).

Measurement and visualisation: After the orthocorrection, 3D measurements were taken in the ERDAS IMAGINE Stereo Analyst module, since on the orthophotos the surface objects are in their two-dimensional position. Floating cursor was used in the measurement, which can be moved in Z direction in addition to X and Y directions. Three data were measured on all buildings: the street, eaves and roof levels, and roof-types were also described. One way of 3D visualisation in Erdas IMAGINE is the Image Drape. Viewpoint and other parameters can be freely changed. Choosing the adequate elevation data, this provides a possibility for the creation of a simplified 3D image of a district (see Figure 4).

Figure 4 Bird's-eye view generated by VirtualGIS on a district

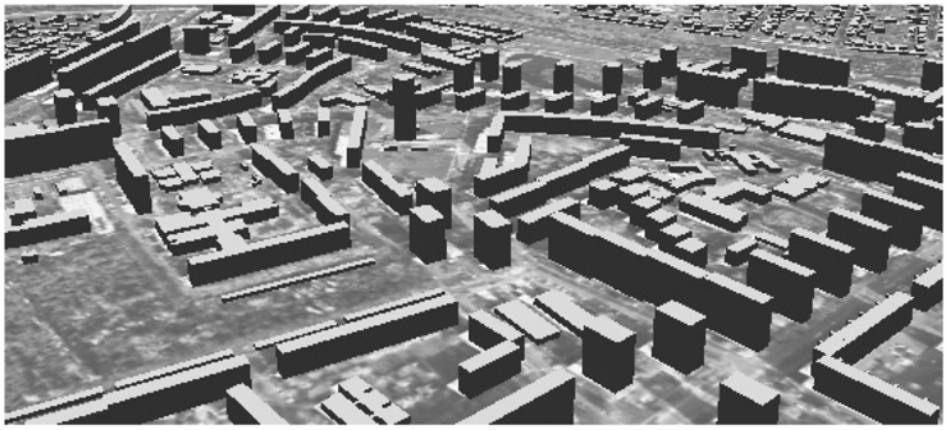

4.1.2 Update and accuracy

In the aerial photos taken in 1992, the newly built large shopping centres did not exist, although they were already included in the plan area database. Since these giant buildings with their extensive parking lots can significantly influence the thermal conditions of their environments, the data-update had primary importance. In this work, the aerial photos of 5 August 2003 were applied. As a result, we earned a data set of surface parameters that is strongly connected in time to the periods of temperature measurements.

For crosschecking, theodolite measurement was also carried out in the cells located at the edge of the study area. Here, the error due to aerial triangulation could be expected to be the greatest, the mean ratio of the differences in value compared to the entire heights of the buildings were around 5%, while the average deviation – based on an element number of almost 100 – was only 58 cm.

4.2 Utilisation of 3D database to the algorithm of the SVF calculation

The 3D database of Szeged includes height data of buildings. This database provides a simplified (‘ideal’) urban surface referring to the shape of buildings, namely all buildings have flat roof, and all walls of a building are of the same height.

The projection of every building on the sky is managed like a projection of their walls visible from a given surface point (see Figure 1). The projection of each edge of the wall is determined by the intersection of the sky and a plane, which is determined by the central point and the visible edge of wall. Thus, in the case of ‘ideal’ urban surface, the shape of the projection of a wall is a globe-quadrilateral bordered by arc sections. All of the wall projections together gives the projection of buildings on the sky hemisphere.

The applied algorithm is similar to the method of integral calculus; it is its adaptation for a hemisphere. Polygon $g(x)$ is the border of the visible sky, under the polygon the sky is not visible because of the building obstruction (Figure 5(a)). After dividing the hemisphere equally into slices by rotation angle, α we draw ‘rectangles’ whose heights are equal to the $g(x)$ values in the middle points of the intervals. The SVF value determined by $g(x)$ polygon is estimated with the sum of the SVF values of these ‘rectangles’ on the hemisphere.

Figure 5 (a) Polygon $g(x)$ as a border of the visible sky and dividing the hemisphere under $g(x)$ equally into slices by angle α (heights are equal to the $g(x)$ values in the middle points of the intervals) and (b) a slice of a ’width’ of α (S) of a basin with an elevation angle β

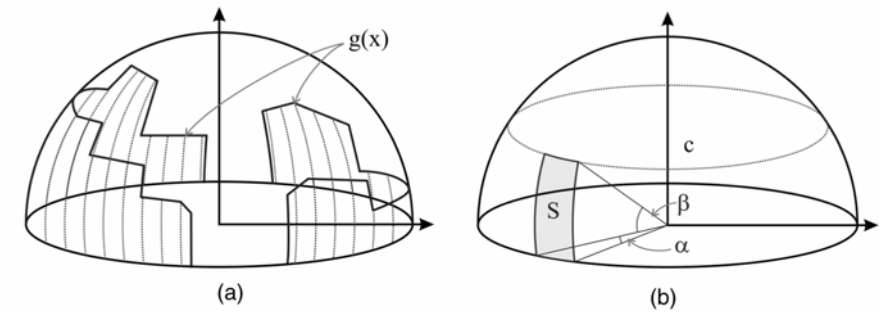

The VF of a basin with an elevation angle β is $\cos^2\beta$ (Formula (1)) and its SVF = $1-\cos^2\beta = \sin^2\beta$, therefore the VF of a 'rectangle' with a 'width' of α (S) is $\cos^2\beta\,(\alpha/360)$ (Figure 5(b)). After adding these values by slices, we subtract the sum from 1 to get the SVF value. The accuracy of the algorithm depends on the magnitude of the selected α. Smaller α angle (finer division) means better estimation of SVF but longer computation time.

The algorithm performs the determination of SVF referred to a surface point in the city as follows. It draws lines by angle α from the selected point and along a line it searches that building which obstructs the largest part from the sky at that direction. It reads the heights of the buildings from the 3D database. After calculating the VF values by lines, it adds them and subtracts the sum from 1 to get the SVF. The length of the lines depends on the user's decision. The obtained SVF values are listed in a table.

4.3 Selection of the appropriate software, program construction, testing

The ESRI ArcView 3.2 software (www.esri.com), which has a built-in and object-oriented language (Avenue) is appropriate for our purpose. With the help of this language, the software is programmable so that every element of the program is accessible (e.g. Souza et al., 2003, 2004).

The constructed application is compiled from nine scripts. Every script fulfils one smaller task (graphical surface, control of the parameters calculation of SVF, etc.). The extension svf_alg.avx is composed from these scripts. Figure 6 illustrates the schematic description of the developed algorithm.

Figure 6 Schematic description of the algorithm

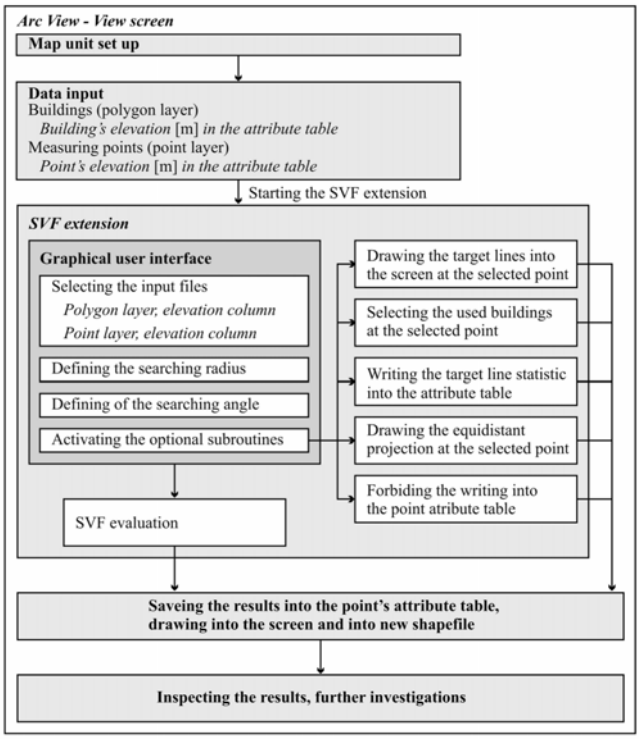

The algorithm was checked by the calculation of two special SVF values (for basin and for 'infinite' long canyon). Firstly, the algorithm ran with a polygon that represented a basin of which the elevation angle was selected randomly. The difference between the SVF values calculated by the Formula (1) and by the algorithm was 0.4%. Secondly, substituting the 'infinite' long canyon with two finite polygon, the difference obtained (with a radius of 2000 m and an interval of 1°) was only 0.01%.

We selected two sites for test running of the algorithm. One is located in a relatively open urban environment, and the other in a more closed area (Figure 7). The selected radius of the investigated area and angle interval of rotation were 200 m and 2°, respectively. The running of the algorithm is finished in about 10 sec. The obtained SVF values were 0.9795 and 0.5758. The explanation of the different values is clearly shown in Figure 7. In the first case, the site is located in a square where the bordering building is not too high. In the second case, the site is in a narrow street bordered by high buildings, therefore its SVF value is significantly lower than that of the first site.

Figure 7 Graphical results of the extension in two different points of the city using 3D building data within a circle

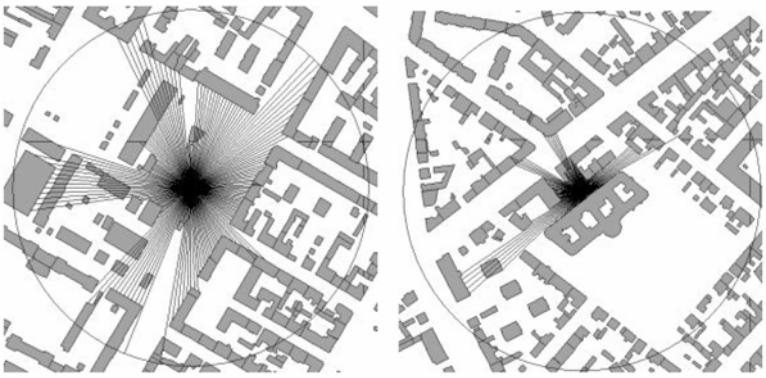

4.4 Selection of the parameters for the algorithm

According to Figure 6, values for two parameters have to be selected. These are the radius of the area around the site in the city where the algorithm takes the building heights and positions into consideration and the interval of the rotation angle, which determines the density of the target lines starting from the site.

In our case, a radius of 200 m seemed to be appropriate. In order to support this value, three sites representing different built-up areas in the city were selected. In the case of radius of 100 m, 31.6%, 85.2% and only 2.5% of the target lines reached buildings around the selected sites, respectively. For a radius of 200 m, the situation improved significantly, the percentage values are 97.7%, 93.3% and 71.6%. Moreover, in the case of a radius of more than 200 m the effect of the radiation process (mentioned in Section 1) in the formation of urban thermal environment around the selected site is negligible because of the absorption and scattering of the more or less polluted air between the buildings.

Selection of a rotation angle of 1° can be explained by two facts. On the one hand, in this case the calculation time is not too long; note that the SVF calculation is necessary for several hundred (or over thousand) points over the whole study area. On the other

hand, an angle of 1° at a distance of 200 m means a width of 3.5 m, so only very narrow buildings could be 'invisible' for the target lines. The effect of such narrow buildings on the radiation processes is also negligible.

In order to refine the described SVF approximation, there is more work to be done, for instance to compare this method with fisheye technique and to investigate the impact of varying angle width and radius, etc.

5 Study area (Szeged), temperature measurements

5.1 Study area

Szeged is located in the southern part of the Great Hungarian Plain at 79 m above sea level on a flat plain (Figure 8). The surface is characterised by Holocene sediments with low relief. According to Trewartha's classification Szeged belongs to the climatic type D.1 (continental climate with longer warm season), similarly to the predominant part of the country. While the administrative area of Szeged is 281 km^2, the inner city is only around 30 km^2, and the densely built-up areas are located inside the circle dike. The avenue-boulevard structure of the town was built to the axis of the river Tisza. The population is 160,000.

Figure 8 Generalised built-up types of Szeged: (a) agricultural and open area, (b) warehouses and industrial area, (c) 1–2 storey detached houses, (d) 5–11 storey block-houses and (e) city core with 3–5 storey buildings; the investigated area and the grid network: (f) border of the investigated area and (g) circle dike

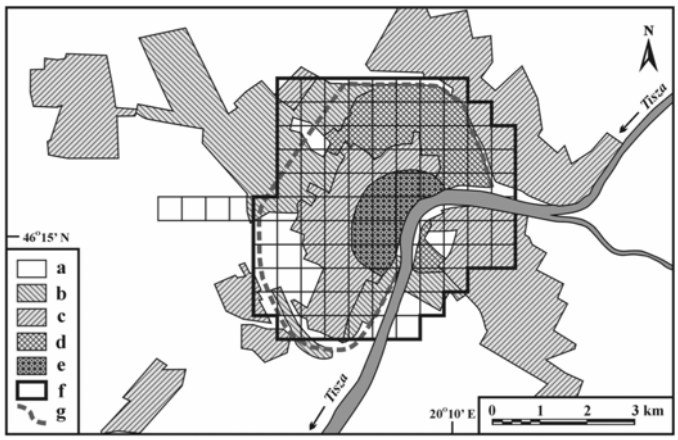

5.2 Temperature measurements

The study area was divided into two sectors and subdivided further into 500 m × 500 m cells (Figure 8). It consists of 107 cells covering the urban and suburban parts of Szeged (26.75 km^2). The outlying parts of the city, characterised by villages and rural features, are not included in the grid, with the exception of four cells on the western side of the area. This latter part was taken in order to determine urban–rural temperature contrasts.

Mobile measurements were taken by two cars in two sectors at the same time on fixed return routes during a one-year period, 35 times altogether. Moving observation in

ΔT detection with different vehicles (car, tram, helicopter, airplane) is a widespread process (e.g. Klysik and Fortuniak, 1999; Moreno-Garcia, 1994; Santos et al., 2003). The approximate 10-day frequency of car traverses provided sufficient information under different, but rainless weather conditions.

Return routes of about 3 hr through all cells by sectors were taken to make time-based corrections. Readings were obtained using radiation-shielded resistance sensors connected to data loggers. A major advantage of studying UHI is that the quantity, of interest, is not the absolute urban temperature, but the difference between urban and rural areas (Streutker, 2003). The possible error in accuracy of sensor is systematic and is thus removed in the differencing procedure. Data were collected every 10 sec, so at a car speed of 20–30 km hr^{-1} the distance between measuring points was 55–83 m. Sensors were mounted at 1.45 m above ground. The logged values at forced stops were deleted from the data set. Having averaged the 15–20 measurement values by cells, time adjustments to a reference time (4 hr after sunset, namely the likely time of the strongest ΔT in the diurnal course, based on earlier measurements) were applied. ΔT values were determined by cell averages (T_{cell}) referring to the temperature average of the westernmost cell ($T_{cell(W)}$) of countryside location (e.g. Lowry, 1977; Unger, 2004; Unger et al., 2001):

$$\Delta T = T_{cell} - T_{cell(W)}$$

This cell consists of agricultural land, mainly non-irrigated wheat, sunflower and maize fields, representative of the rural surroundings (see Figure 8).

6 Selection of the representative sample area

The geometric survey of the whole town would take enormous effort and time due to the high number of buildings (about 22,000). Thus, only a selected sample area was studied in detail, and we draw our conclusions on the basis of the building data obtained from this smaller though highly representative area.

6.1 Stratified sampling

Stratified sampling is a sampling design in which prior information about the population is used to determine groups (called strata) that are sampled independently. Each possible sampling unit or population member belongs to exactly one stratum. There can be no sampling units that do not belong to any of the strata and no sampling units that belong to more than one stratum. When the strata are constructed to be relatively homogeneous with respect to the variable being estimated, a stratified sampling design can produce estimates of overall population parameters (e.g. mean, proportion) with greater precision than estimates obtained from simple random sampling.

If the investigator has prior knowledge of the spatial distribution of the study area, the strata should be defined so that the area within each stratum is as homogeneous as possible. The variable providing the information used to establish the strata (that is the so-called ‘auxiliary variable’) was the built-up ratio.

The strata should be determined before allocating the sample sizes. When the strata are defined according to an auxiliary variable that is correlated with the variable to be estimated, the optimal definition of the strata is that the population included in each

stratum should be as homogeneous as possible with respect to the auxiliary variable. If there is a particular interest of estimating the overall mean for the population, Cohran (1963) suggests defining no more than six strata and using a procedure attributed to Dalenius and Hodges (1959) to determine the optimal cut-off values for each of the strata, based on the distribution of the auxiliary variable for the population. In this study, six strata have been defined and the numbers of elements in samples by strata have been determined. Table 1 shows the final result of defining the six strata.

Table 1 Number of cells in each stratum and in each sample (Labels 1 and 6 mean strata containing the least and the best built-up cells, respectively)

Label of stratum	*In stratum*	*In samples*
1	11	4
2	14	5
3	18	6
4	20	7
5	22	7
6	18	6
Total	103	35

6.2 Selection based on spatial distribution

When selecting the appropriate cells from the strata, the priority is to find the most balanced distributions. Moreover, it is also important to include some specific parts of the town with significant temperature anomaly, where surface conditions suddenly change.

In selection we had several adequate alternatives, but only those were kept, in which cases the mean heat island field – interpolated from the data of 35 cells – was the closest to the mean field constructed from the values of 103 cells, both from a structural and intensity point of view. As a result of this process, cells of the chosen sample area have relatively scattered location within the whole research area (Figure 9). In those places where the chosen cells are located near each other, the horizontal temperature gradient was high at the time of development of the UHI.

Figure 9 Distribution of the cells of the sample area in the investigated area: (a) border of the investigated area and (b) cells not included in the sample area, (1–6) cells selected from the given strata (see text and Table 1)

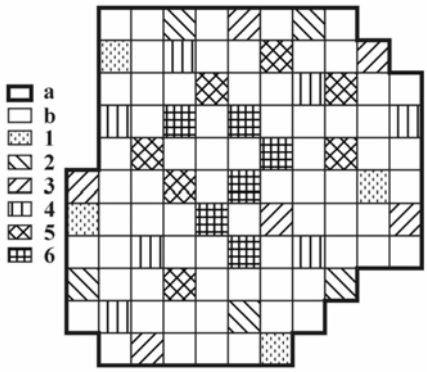

7 Calculation of the SVF and its relationship with the air temperature in Szeged

7.1 The running of the algorithm

SVF values for the sites in 35 cells of the selected sample area were determined by applying the developed algorithm. In order to do this, first the measurement route running along the middle of the streets had to be localised on the digital map of the city containing the plan areas of buildings (Figure 10). The resolution of the SVF calculation along the route was 20 m. This point density secures the representativity of the obtained SVF value for a given cell by averaging the SVF values calculated in that cell. The elevation of each point was obtained from the earlier-mentioned DEM. One of the results of the algorithm is a drawing in equiangular projection (like fisheye images) on sky obstruction caused by the buildings around the selected point (Figure 11).

Figure 10 Building plan areas data in a selected part of the city with a section of the measurement route (a – temperature and SVF measurement route, b – SVF measurement points, c – site of the measurement point in Figure 11)

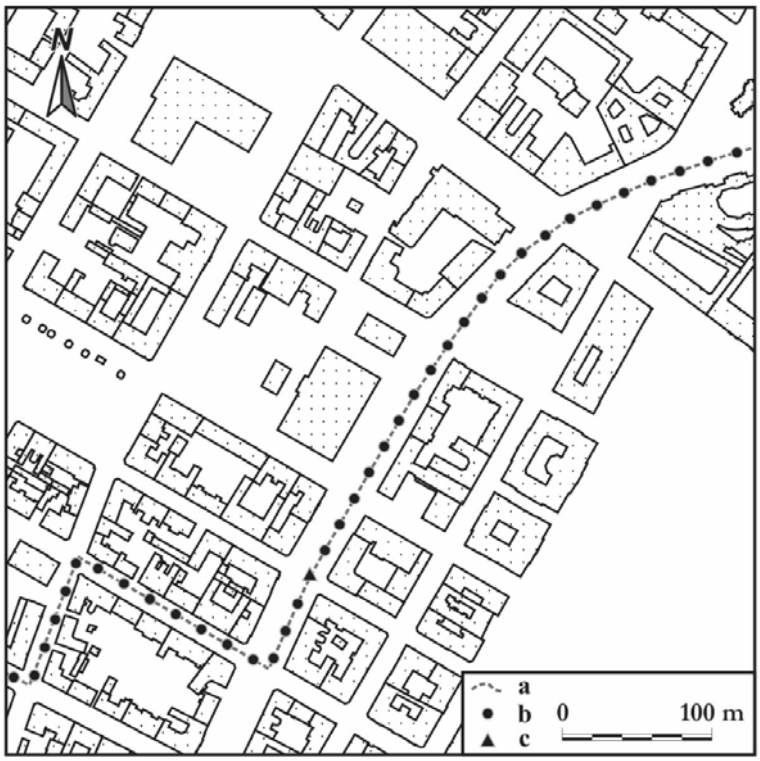

For every point (a total of 1022), the scanned areas have a radius of 200 m and a rotation angle of 1°. The algorithm was applied not only for the ground level but also for a height of 1.4 m above ground level, because the temperature values were also measured at this level (Svensson, 2004). For the whole sample area the total running time was about 10 hr. Then the average SVF values were calculated by cells.

Figure 11 Sky obstruction around the point marked by ▲ in Figure 10 in equiangular projection (like fisheye photograph) (SVF = 0.7722)

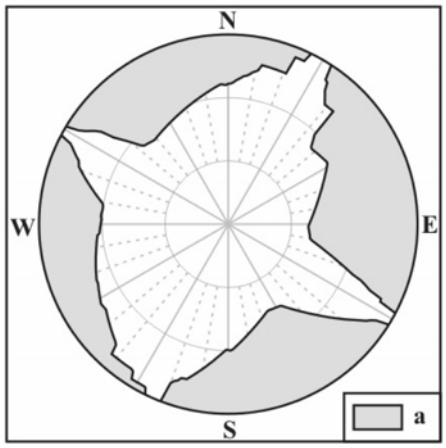

7.2 *Connection between UHI and SVF in different seasons and in different heights*

In this section, a relatively new process is applied to examine the surface geometry–air temperature connection within an urban area concerning the utilisation of areal means of UHI intensity (ΔT) and SVF (Blankenstein and Kuttler, 2004; Unger, 2004) as element pairs in a statistical investigation using linear regression. The difference in the strength of relationships between SVF determined for different levels above ground and air temperature is also examined.

This study on the influence of SVF on intra-urban temperature distribution is more comprehensive than the previous ones because the obtained data set represents almost the entire urban area, the number of element pairs used for comparison is relatively large (35) and the cell areas (0.25 km^2) are not too small, so the selected scale of the investigated urban units is not micro- but rather topo-scale.

Earlier investigations showed that highest ΔT values were found for cells in the centre of Szeged than in the suburbs (e.g. Unger et al., 2001, 2004). It is generally true that cells located at the city border have high mean SVF values and cells located near the centre have low mean SVF values. On the contrary, among the sampled cells in Szeged there are cells with low SVF values at the city border because large housing estates with high rise buildings are located. Because of this complex situation, we do not take the distance to the city border into account and put all cases into one regression relation.

According to our expectations, the connection between SVF and ΔT averages will be stronger in the leaf-off (heating) season, because our estimation on SVF is based only on building geometry and it shows more connection with the real SVF situation in the colder than in the warmer (and greener) half-year.

The applied parameters (as cell averages) are the following:

- *Independent variable*: SVF (ground level, 1.4 m above ground level).
- *Dependent variable*: UHI intensity (1.4 m above ground level, year, non-heating and heating seasons).

Firstly, we examine the relationship between SVF at two levels and the one-year average of ΔT calculated from 35 night measurements at the time of its best expression (see Section 5.2). The effects of different weather situations (favourable and not favourable for heat island development) are amalgamated in these ΔT averages. Secondly, we study the relationships in the leaf-off (heating) and the leaf-on (non-heating) seasons separately. Finally, we compare the difference in relationships using SVF values at two different heights. Naturally, the cell means of SVF are the same in all cases, because the surface elements practically did not change in the one-year study period. Their values range between 0.73 and 1.00 at ground level and between 0.76 and 1.00 at a height of 1.4 m in the centre and at the outskirts, respectively.

In the one-year period, mean ΔT ranges between 0.74°C and 2.72°C inside the sample area. The highest ΔT values occur in the central parts, almost in the geometrical centre of the investigated area. Figure 12 shows a strong linear connection between SVF and ΔT in the studied urban area. According to the obtained statistical measures, the intra-urban variations of temperature excess can be explained by the variations of SVF at ground level in 42.6% and at 1.4 m above ground level in 44.1%. The correlation coefficients are –0.653 and –0.664 which mean strong negative relationships at 1% significance level (n = 35) (Table 2). Thus, a slight improvement of the coefficient of determination was obtained when using $SVF_{1.4}$.

Figure 12 Connection between the SVF at two different levels and the annual mean UHI intensity (ΔT) (2002–2003) (n = 35)

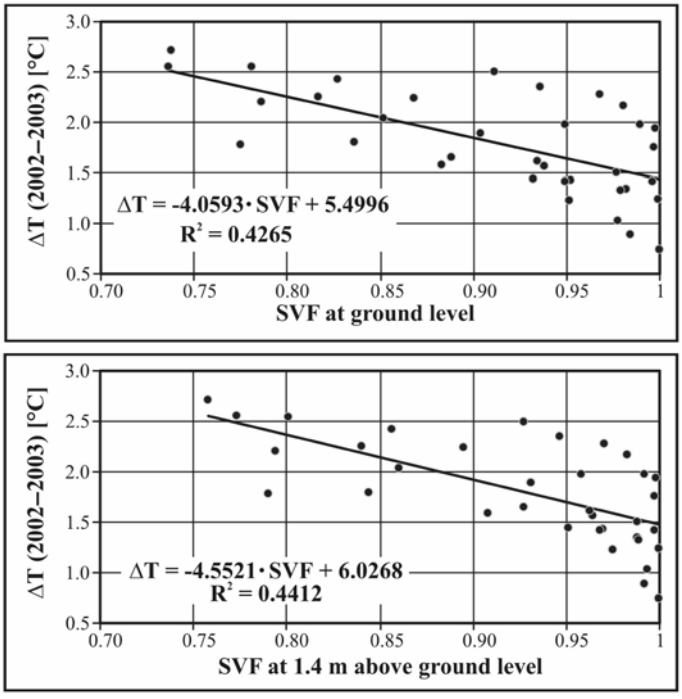

The highest ΔTs in the leaf-off and leaf-on seasons range between 0.85–2.63°C and 0.64–2.79°C, respectively. The comparison between the colder and warmer half-years revealed that the connection was stronger (at a significance level of 1%) in the colder

season than in the warmer season at both level as it was expected, but the difference is not too large. The calculated linear regression equations and their characteristics are given in Table 2. These relationships are valid within the ranges of the investigated parameters.

Table 2 Relationships between annual mean (ΔT_y), heating season's mean (ΔT_h) and non-heating season's mean (ΔT_{nh}) UHI intensity and Sky View Factor at ground level (SVF_g) and at a height of 1.4 m ($SVF_{1.4}$), as well as correlation coefficients (r), coefficients of determination (R^2) and levels of significance ($n = 35$)

Case	*Regression equation*	*R*	R^2	*Significance level (%)*
Year, ground level	$\Delta T_y = -4.059SVF_g + 5.499$	–0.653	0.4265	1
Heating season, ground level	$\Delta T_h = -4.268SVF_g + 5.615$	–0.656	0.4309	1
Non-heating season, ground level	$\Delta T_{nh} = -3.862SVF_g + 5.390$	–0.632	0.3991	1
Year, 1.4 m	$\Delta T_y = -4.552SVF_{1.4} + 6.026$	–0.664	0.4412	1
Heating season, 1.4 m	$\Delta T_h = -4.808SVF_{1.4} + 6.189$	–0.671	0.4498	1
Non-heating season, 1.4 m	$\Delta T_{nh} = -4.310SVF_{1.4} + 5.873$	–0.639	0.4089	1

The correlation coefficients of –0.656 (–0.671) and –0.632 (–0.639) indicated negative relationships, which mean only a seasonal difference of 2.2% and 3.2% in the explanation of ΔT variation caused by the variation of SVF at ground level and at a height of 1.4 m, respectively. These slight differences show a small influence of the summer tree canopies on the seasonal variation of SVF. One would expect less outgoing long wave radiation in areas with foliated trees because of the additional obstruction effect of the vegetation in a mixed urban environment with buildings and trees, resulting in higher temperatures. However, it is possible that the smaller SVF values result in smaller insolation as a result of altered shadow patterns during daytime, which may influence the air temperature at night. In the present stage of our investigation, we assume that the influence of the foliated trees on ΔT along the measurement routes is minor comparing to the obstruction effect of buildings, which is the same in both season.

Thus, there is no significant difference in the influence of the SVF on the ΔT variations of differently vegetated seasons in the study area. The small differences in favour of leaf-off case indicate a minor effect of tree conditions on our process for the estimation of SVF in the study area. It is interesting to note that weaker relationships cannot be experienced in the one-year 'all-weather' period. This may mean that the features of urban surface geometry influence (even in 'less favourable' weather conditions) the intra-urban temperature distribution to a great extent. These results are similar to the results in Unger (2004) where the SVF estimation was carried out by analytical method.

According to our results, SVF data from an elevation of 1.4 m are better to use for regression analysis than values belonging to the ground level. This is in contrast with the results obtained by Svensson (2004) (see Section 3), which can be attributed to the difference in the areal extensions of the investigated parameters. This apparent contradiction is derived from the different approaches. Svensson (2004) compared the

variables referring to individual sites, while we used areal means, where the areas extended over several blocks in the city. In our case the surface geometry of the immediate surroundings around the measurement sites is not so dominant on the obtained areal temperature value because it is influenced by different surroundings, which means their effects on areal average ΔT are balanced and equalised.

8 Conclusions

Concerning the SVF–ΔT relationship, the obtained results found in the literature are rather contradictory. These investigations were restricted to specific parts of cities and used small numbers of sites and few occasions of measurements. In this way, any examination of possible connections were also based on a small number of element pairs. Comparisons were often based on element pairs measured at some selected sites. In some cases we can meet with areal means as well, nevertheless always in the case of one of the examined variables. Two exceptions are provided by the works of Blankenstein and Kuttler (2004) and Unger (2004).

For comparison, our study utilised a large number of areal means of SVF and ΔT. Values were related to a large sample area and based on numerous measurements. The sample area was selected by the method of stratified sampling. According to the results, there is a strong relationship between the intra-urban variations of these variables. That means that urban surface geometry (described by SVF) is a significant determining factor of the air temperature distribution inside the city.

Thus, after summarising the results of international and recent investigations in Szeged, we can conclude that while searching for the connections between urban geometry and temperature in a more adequate way, further studies should be based on areal approach, that is, on comparison of areal means. Measured values at sites might show large variations because of the influence of micro-variations of the immediate environments. Moreover, measured temperature values can be affected by advective effects from the wider environment (source area). Therefore, the first step of the investigation should be the selection of a proper scale. The application of areal means referred to an appropriate-sized urban area (e.g. a larger block) should gather and summarise the effects of micro-scale processes and should reveal the summarised results (values) representative for the given area. Also, investigation of a sufficient number of appropriate-sized areas covering the largest part of a city or the entire city is needed to draw well-established conclusions on the studied relationship.

Acknowledgements

This research was supported by the Hungarian Scientific Research Fund (OTKA T/049573). The author wishes to give special thanks to the reviewers for their helpful comments, to the Division of Geodesy and Cartography (Hungarian Ministry of Agricultural and Rural Development) for the aerial photo negatives, to the Town Council of Szeged for providing the digital building plan area database of Szeged, to T. Gál, J. Geiger and Z. Sümeghy (Univ. Szeged) for your enormous work in this research. Linguistic revision was carried out by E. Tanács (Univ. Szeged).

References

Blankenstein, S. and Kuttler, W. (2004) 'Impact of street geometry on downward longwave radiation and air temperature in an urban environment', *Meteorologische Zeitschrift*, Vol. 15, pp.373–379.

Bottyán, Z. and Unger, J. (2003) 'A multiple linear statistical model for estimating the mean maximum urban heat island', *Theoretical and Applied Climatology*, Vol. 75, pp.233–243.

Bärring, L., Mattson, J.O. and Lundqvist, S. (1985) 'Canyon geometry, street temperatures and urban heat island in Malmö, Sweden', *Journal of Climatology*, Vol. 5, pp.433–444.

Bradley, A.V., Thornes, J.E. and Chapman, L. (2001) 'A method to assess the variation of urban canyon geometry from sky view factor transects', *Atmospheric Science Letters*, Vol. 2, pp.155–165.

Brown, M.J., Grimmond, C.S.B. and Ratti, C. (2001) 'Comparison of methodologies for computing sky view factor in urban environment', *Internal Report Los Alamos National Laboratory*, Los Alamos, NM, LA-UR-01-4107.

Brown, M.J. and Grimmond, C.S.B. (2001) 'Sky view factor measurements in downtown Salt Lake City', *Data Report for the DOE CBNP Experiment, October 2000: Internal Report Los Alamos National Laboratory*, Los Alamos, NM, LA-UR-01-1424.

Chapman, L. and Thornes, J.E. (2004) 'Real-time sky-view factor calculation and approximation', *Journal of Atmospheric and Oceanic Technology*, Vol. 21, pp.730–741.

Chapman, L., Thornes, J.E. and Bradley, A.V. (2001) 'Rapid determination of canyon geometry parameters for use in surface radiation budgets', *Theoretical and Applied Climatology*, Vol. 69, pp.81–89.

Chapman, L., Thornes, J.E. and Bradley, A.V. (2002) 'Sky-view factor approximation using GPS receivers', *International Journal of Climatology*, Vol. 22, pp.615–621.

Cohran, W.G. (1963) *Sampling Techniques*, 2nd edition, New York: John Wiley & Sons.

Dalenius, T. and Hodges Jr., J.L., (1959) 'Minimum variance stratification', *Journal of the American Statistical Association*, Vol. 54, pp.88–101.

Eliasson, I. (1996) 'Urban noctural temperatures, street geometry and land use', *Atmospheric Environment*, Vol. 30, pp.379–392.

Goh, K.C. and Chang, C.H. (1999) 'The relationship between height to width ratios and the heat island intensity at 22:00 h for Singapore', *International Journal of Climatology*, Vol. 19, pp.1011–1023.

Golany, G.S. (1996) 'Urban design morphology and thermal performance', *Atmospheric Environment*, Vol. 30, pp.455–465.

Grimmond, C.S.B., Potter, S.K., Zutter, H.N. and Souch, C. (2001) 'Rapid methods to estimate sky-view factors applied to urban areas', *International Journal of Climatology*, Vol. 21, pp.903–913.

Holmer, B. (1992) 'A simple operative method for determination of sky view factors in complex urban canyons from fisheye photographs', *Meteorologische Zeitschrift*, N.F. Vol. 1, pp.236–239.

Holmer, B., Postgård, U. and Eriksson, M. (2001) 'Sky view factors in forest canopies calculated with IDRISI', *Theoretical and Applied Climatology*, Vol. 68, pp.33–40.

Johnson, D.B. (1985) 'Urban modification of diurnal temperature cycles in Birmingham, UK', *Journal of Climatology*, Vol. 5, pp.221–225.

Johnson, G.T. and Watson, J.D. (1984) 'The determination of view-factors in urban canyons', *Journal of Climate and Applied Meteorology*, Vol. 23, pp.329–335.

Klysik, K. and Fortuniak, K. (1999) 'Temporal and spatial characteristics of the urban heat island of Lódz, Poland', *Atmospheric Environment*, Vol. 33, pp.3885–3895.

Kuttler, W. (2005) 'Stadtklima', in P. Hupfer and W. Kuttler (Eds). *Witterung und Klima*, Teubner, Stuttgart-Leipzig-Wiesbaden, Germany, pp.371–432.

Landsberg, H.E. (1981) *The urban climate*, New York: Academic Press.

Lindberg, F. (2004) 'Towards the use of local governmental 3-D data within urban climatology studies', *Mapping and Image Science*, Vol. 2, pp.4–9.

Lowry, W.P. (1977) 'Empirical estimation of urban effects on climate: a problem analysis', *Journal of Applied Meteorology*, Vol. 16, pp.129–135.

Moreno-Garcia, M.C. (1994) 'Intensity and form of the urban heat island in Barcelona', *International Journal of Climatology*, Vol. 14, pp.705–710.

Oke, T.R. (1981) 'Canyon geometry and the nocturnal urban heat island: comparison of scale model and field observations', *Journal of Climatology*, Vol. 1, pp.237–254.

Oke, T.R. (1987) *Boundary Layer Climates*, London and New York: Routledge.

Oke, T.R. (1988) 'Street design and urban canopy layer climate', *Energy and Buildings*, Vol. 11, pp.103–113.

Park, H-S. (1987) 'Variations in the urban heat island intensity affected by geographical environments', *Environmental Research Center Papers*, Vol. 11, The University of Tsukuba, Ibaraki, Japan, p.79.

Santos, I.G., Lima, H.G. and Assis, E.S. (2003) 'A comprehensive approach of the sky view factor and building mass in an urban area of the city of Belo Horizonte, Brazil', in K. Klysik, T.R. Oke, K. Fortuniak, C.S.B. Grimmond and J. Wibig (Eds) *Proceedings of Fifth International Conference on Urban Climate*, Vol. 2, University of Lodz, Lodz, pp.367–370.

Souza, L.C.L., Pedrotti, F.S. and Leme, F.T. (2004) 'Urban geometry and electrical energy consumption in a tropical city', *Proceedings Fifth Conference on Urban Environment*, AMS Meeting, Vancouver, CD 4.10.

Souza, L.C.L., Rodrigues, D.S. and Mendes, J.F.G. (2003) 'The 3DSkyView extension: an urban geometry access tool in a geographical information system', in K. Klysik, T.R. Oke, K. Fortuniak, C.S.B. Grimmond and J. Wibig (Eds). *Proceedings of the Fifth International Conference on Urban Climate*, Vol. 2, University of Lodz, Lodz, Poland, pp.413–416.

Steyn, D.G. (1980) 'The calculation of view factors tron fisheye-lens photographs', *Atmosphere-Ocean*, Vol. 18, pp.254–258.

Steyn, D.G., Watson, I.D., Johnson, G.T. and Hay, J.E. (1986) 'The determination of sky-view factors in urban environments using video imagery', *Journal of Atmospheric Oceanic Technology*, Vol. 3, pp.759–764.

Streutker, D.R. (2003) 'Satellite-measured growth of the urban heat island of Houston, Texas', *Remote Sensing Environment*, Vol. 85, pp.282–289.

Svensson, M. (2004) 'Sky view factor analysis – implications for urban air temperature differences', *Meteorology Applications*, Vol. 11, pp.201–211.

Unger, J. (2004) 'Intra-urban relationship between surface geometry and urban heat island: review and new approach', *Climate Research*, Vol. 27, pp.253–264.

Unger, J., Bottyán, Z., Sümeghy, Z. and Gulyás, Á. (2004) 'Connections between urban heat island and surface parameters: measurements and modeling', *Idõjárás*, Vol. 108, pp.173–194.

Unger, J., Sümeghy, Z., Gulyás, Á., Bottyán, Z. and Mucsi, L. (2001) 'Land-use and meteorological aspects of the urban heat island', *Meteorology Applications*, Vol. 8, pp.189–194.

Upmanis, H., Eliasson, I. and Lindquist, S. (1998) 'The influence of green areas on nocturnal temperatures in a high latitude city (Göteborg, Sweden)', *International Journal of Climatology*, Vol. 18, pp.681–700.

Vieira, H. and Vasconcelos, J. (2003) 'Urban morphology characterisation to include in a GIS for climatic purposes in Lisbon: discussion of two different methods', in K. Klysik, T.R. Oke, K. Fortuniak, C.S.B. Grimmond and J. Wibig (Eds). *Proceedings of Fifth International Conference on Urban Climate*, Vol. 2, University of Lodz, Lodz, pp.417–420.

Watson, I.D. and Johnson, G.T. (1987) 'Graphical estimation of sky view-factors in urban environments', *Journal of Climatology*, Vol. 7, pp.193–197.